PROCEEDINGS OF ECOS 2023 - THE 36TH INTERNATIONAL CONFERENCE ON
EFFICIENCY, COST, OPTIMIZATION, SIMULATION AND ENVIRONMENTAL IMPACT OF ENERGY SYSTEMS
25-30 JUNE, 2023, LAS PALMAS DE GRAN CANARIA, SPAIN

# Robust Optimization of the Energy Concept of an Industrial Process w.r.t. Uncertain Energy Costs and Environmental Conditions

***Michael Lockan[a], Rushit Kansara[a]***

*[a] German Aerospace Centre (DLR),*
*Institute of Low-Carbon Industrial Processes, Cottbus, Germany,*
*michael.lockan@dlr.de*

**Abstract:**

Due to the required $CO_2$ reduction to achieve global climate goals, the political, social, and economic pressure for decarbonizing industry increases rapidly. An essential step towards this goal is the replacement of fossil fuels by renewable energy sources making changes in technology for generating electricity, steam, and process heat an inevitable requirement. This raises the question about the combination of energy supply technologies (such as photovoltaic systems, wind turbines or solar thermal systems) with energy conversion units (such as heat pumps or electric boilers) to cover the demand of an industrial process at minimal cost. Optimization methods are increasingly used for the selection and dimensioning of such units. These methods can systematically and efficiently determine optimal energy concepts according to the multicriterial requirements of a specific industrial process.

The results of such deterministic optimizations depend heavily on assumptions of environmental conditions such as solar radiation and wind speed, the cost of purchasing and selling revenue of electric power, local infrastructure, and the demand of the industrial plant. Changes in these assumptions can result in significantly different costs or lead to an energy system, which is eventually incapable of covering the process demand. In this paper, the modelling of the required components is briefly described and a robust optimization approach is presented taking uncertainties of the assumptions into account during the optimization process. After a robust optimization for an industrial process is performed, the results are compared and discussed to those of a deterministic optimization. It can be shown, that the robust optimization allows to find energy concepts with less sensitivity and higher reliability when uncertainties are considered.

**Keywords:**

decarbonization of industry, energy concept, robust optimization, component modelling.

## Nomenclature

$A$ area [$\mathrm{m}^2$]
$C$ capital expenditures [€]
$c$ constant, specific heat [kJ/(kg K)]
$E$ energy [kWh]
$f$ performance, uncertainty factor [-]
$g$ specific global warming index [$\mathrm{g_{CO2eq}/kWh}$]
$\dot{m}$ mass flow rate [kg/s]
$m$ mass [kg]
$P$ power [kW], probability, quantile [-]
$p$ specific price [€/kWh]
$\mathbf{p}$ parameter vector [-]
$Q$ thermal energy [kWh]
$\dot{Q}$ thermal power [kW]
$S$ solar radiation [kWh/($\mathrm{m}^2$)]
$T$ temperature [K]

**Abbreviations**

EB electric boiler
GB gas boiler
GWI global warming index
HP heat pump
PV photovoltaic
ST solar thermal unit
TAC total annual cost
TES thermal energy storage
WT wind turbine

**Greek symbols**

$\alpha$ maintenance factor
$\beta$ panel tilt angle, interest rate
$\gamma$ scaling exponent
$\delta$ declination angle of the sun
$\eta$ efficiency
$\tau$ time horizon
$\lambda$ load fraction
$\varphi$ latitude industrial site

**Subscripts and superscripts**

$d$ daily
$det$ deterministic
$hor$ horizontal
$in$ inlet
$inc$ incidence
$nom$ nominal
$out$ output
$pan$ penal
$rob$ robust


https://doi.org/10.52202/069564-0123

# 1. Introduction

For a successful decarbonization of industrial processes it is essential to integrate renewable energies in an appropriate way considering economic as well as environmental aspects. For this purpose, it is necessary to model the required units of the considered process and the energy concept sufficiently to gain an understanding of their interaction and characteristics. Due to the huge number of parameters involved describing an energy concept it is necessary and to use numerical optimization strategies in order to find optimal configurations.

## 1.1. Optimization of energy concepts

With the increasing complexity of the investigated systems and the associated number of parameters to be defined, as well as with increasing requirements, optimization processes are increasingly used. This includes almost all industrial areas in which designs and systems are consistently pushed to the limits of feasibility. Thus, the need for design and operational optimizations of energy concepts for industrial processes is also increasing due to the global economic competition and increasing political and social pressure to reduce $CO_2$ emissions. The design of an energy concept is typically formulated as mixed integer nonlinear problem, where the nominal capacity of the units is described by real number whereas with the integer variable the number of units used defined, [1]. In the context of this paper, the units used are specified, so that the complexity of the optimization problem can be reduced, while still using nonlinear modelling of the units, *Figure 1*. A more accurate unit modelling is usually used for operational optimizations involving e.g. non-linear model predictive control with real-time weather data or forecasts, [2]. Such a complex operational optimization is not carried out here, but a simplified operational optimization is need to determine the operating costs, which results in a two-level optimization problem. Thus, a stationary modelling of the components is sufficient for the design optimization of the energy concept.

## 1.2. Robust optimization strategies

Optimized systems often only behave ideally under the given boundary conditions, so that deviations can lead to undesired system behaviour or a loss of performance. The goal of a robust optimization is to consider uncertainties or possible deviations directly during design optimization process. There are many definitions regarding robustness, like a small scatter in the objectives or low failure probabilities, [3]. For each of the defined robust criteria there are sophisticated methods for their efficient estimation. In any case, the consideration of conditions away from the design point requires a number of function evaluations to determine the robust objectives. To avoid this, usually only selected scenarios are considered in current energy concept design processes [4]. However, response surface methods in connection with robust optimizations are often very suitable, which can be created on the basis of a few function evaluations and then used to carry out extensive statistical evaluations efficiently [5]. In this paper local response surfaces are used for the robust optimization of an energy concept, which are created around the design point in every design evaluation.

## 1.3. Structure of the paper

In the following section the mathematical modelling of the units under consideration is described and the corresponding analysis of the entire energy concept is explained*, Figure 1*. An electrical batterie is not directly considered in this paper, but since the energy balances are calculated on a daily basis, it is assumed that the corresponding amount of electricity can be stored for a short time. The unit modelling serves as the basis for the energy concept design process, in which the nominal capacities of the units are optimized. Finally, the robust optimization problem is presented and its solution is compared with a deterministic optimum.

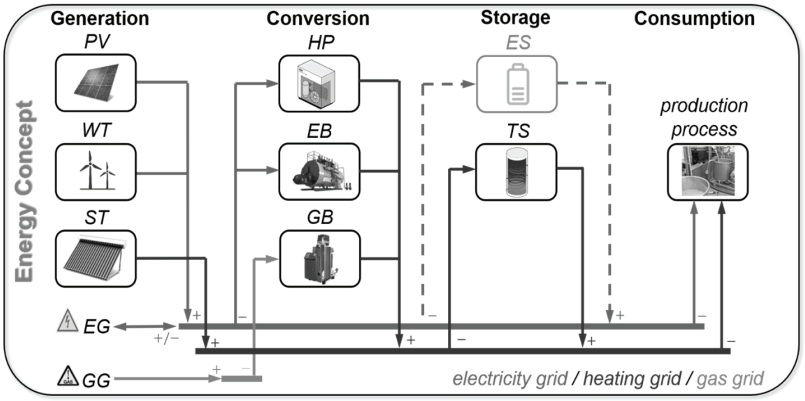


**Figure 1** *overview of the energy concept to be optimized showing the electricity, gas and heating grid*

https://doi.org/10.52202/069564-0123

## 2. Modelling of the energy concept

In order to design and dimension the units shown in *Figure 1*, it is necessary to model them by an energetic point of view. The modelling then forms the basis for determining the electrical energy and heat produced in order to cover the production needs at all times. For this purpose, the formulations of the generation, conversion and storage units are first described in the following sections before the evaluation of the overall system is explained.

### 2.1. Generation units

The output of the generation units essentially depends on the installed capacity, solar radiations and wind speeds. The installed capacity is described by the area of the panels for the PV and ST units and by the nominal power for the wind turbine. The electrical power $P^{PV}$ provided by the PV unit is thus calculated according to [2] by

$$P^{PV} = A^{PV}\eta^{PV}S^{pan} \tag{1}$$

with the unit area $A^{PV}$, penal efficiency $\eta^{PV}$ and solar radiation $S^{pan}$ which summarizes direct and diffuse radiations. The electrical power is limited by the nominal capacity $P^{PV}_{nom}$, such that

$$P^{PV} \leq P^{PV}_{nom} \qquad \text{with} \qquad P^{PV}_{nom} = A^{PV}P^{PV}_{nom,rel} = A^{PV}0.171. \tag{2}$$

Values for solar radiation are taken from monthly totals $S^{hor}_{M}$ for a horizontal surface for the region of the industrial site from the DWD, [6]. Using the geometric relationships in *Figure 2a*, the corresponding solar radiation $S^{inc}$ of the sun can be measured using its declination angle $\delta$ as well as the latitude $\varphi$ of the industrial site:

$$S^{inc} = \frac{S^{hor}}{\sin\alpha} \qquad \text{with} \qquad \alpha = 90° - \varphi + \delta. \tag{3}$$

A tilt angle $\beta$ of the PV module then corresponds to a decrease in latitude $\varphi$, so that the solar radiation on the module is calculated by

$$S^{pan} = S^{inc}\,sin(\alpha+\beta) = S^{hor}\frac{sin(\alpha+\beta)}{\sin\alpha}. \tag{4}$$

The efficiency of the PV unit was chosen with $\eta^{PV} = 0.09$ in such a way that calculated values correspond to the measurements of a PV unit already installed at the industrial site.

The electrical power provided by the wind turbine unit is determined by the nominal power $P^{WT}_{nom}$ and a wind load fraction $\lambda^{WT}$ dependent efficiency $\eta^{WT}$:

$$P^{WT} = \eta^{WT}(\lambda^{WT})P^{WT}_{nom} \qquad \text{with} \qquad \lambda^{WT} = \frac{v^{wind}}{v^{wind,0}} \tag{5}$$

where a reference wind speed of $v^{wind,0} = 12ms^{-1}$ is chosen for the present study. Due to the linear dependency in (5), only a single representative wind turbine unit is considered at this point, a separation into several wind turbines with different capacities does not take place here. The efficiency function is selected according to [2]

$$\eta^{WT}(\lambda^{WT}) = \begin{cases} 0 & if \quad \lambda^{WT} < 0.33 \\ 1.5393\lambda^{WT} - 0.5091 & if \quad 0.33 \leq \lambda^{WT} \leq 1.0 \\ 1 & if \quad \lambda^{WT} > 1.0 \end{cases} \tag{6}$$

and displayed *Figure 2b*. The wind speeds used here are taken from measurements at the industrial site. The same distributions of wind speeds and thus the same output of the wind turbine unit is assumed for each day in this paper. A distinction between days with a lot and little wind does not take place for the design of the wind turbine unit.

To determine the output of the solar thermal unit, a single equivalent solar panel is usually considered, for which the inlet and outlet temperatures w.r.t a given the mass flow are calculated, [7]. However, to find an appropriate design an optimization of the mass flow in the panels is required, which may necessary for an operational consideration, but not for the design. For the design, the calculation of the thermal performance

$$\dot{Q}^{ST} = A^{ST}\eta^{ST}_0 S^{pan} f^{ST} \qquad \text{with} \qquad f^{ST} = 0.97 - 0.0367\left(\frac{a^*}{\eta^{ST}_0}\right) + 0.0006\left(\frac{a^*}{\eta^{ST}_0}\right)^2 \tag{7}$$

using the panel area $A^{ST}$, the zero-loss panel efficiency $\eta^{ST}_0$, the solar radiation on the penal $S^{pan}$ as in (4) and a collector performance factor $f^{ST}$, [8]. Heat losses from the panel are considered using the performance


https://doi.org/10.52202/069564-0123

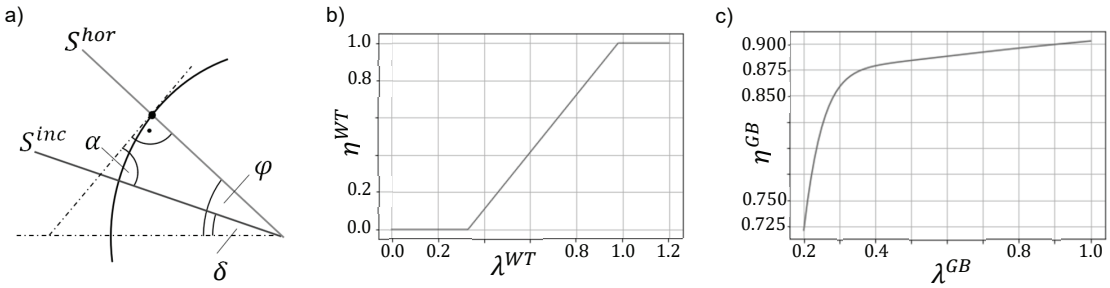


**Figure 2** a) angles to calculate the solar radiation b) efficiency of wind turbines depending on the wind load and c) efficiency of the gas boiler depending on the load fraction

factor $f^{ST}$, which depends on the type of panel. For this paper, evacuated tubes with $\eta_0^{ST} = 0.6$ and $a^* = 3$ are used.

## 2.2. Conversion units

The task of the conversion units is to provide the heat required for the industrial process using electricity or gas. There are a lot of ways to generate heat, e.g. using combined heat and power units, but firstly only the components described below were considered in this work. The thermal output $\dot{Q}^{GB}$ of the gas boiler is calculated according to

$$\dot{Q}^{GB} = \dot{Q}_{nom}^{GB} \lambda^{GB} \tag{8}$$

with the nominal capacity $\dot{Q}_{nom}^{GB}$ and the load fraction $\lambda^{GB}$ limited by lower and upper bounds $0.2 \leq \lambda^{GB} \leq 1.0$ . The power $P^{GB}$ required for generating $\dot{Q}^{GB}$ is calculated based on the efficiency $\eta^{GB}$, so that the behavior in part load can also be considered, [2]:

$$P^{GB} = \frac{\dot{Q}^{GB}}{\eta^{GB}} \quad \text{with} \quad \eta^{GB} = \frac{21.754\lambda^{GB^3} - 7.001\lambda^{GB^3} + 1.397\lambda^{GB} - 0.076}{20.666\lambda^{GB^3} - 5.342\lambda^{GB^3} + 0.678\lambda^{GB} + 0.035} \eta_{nom}^{GB} \tag{9}$$

and a nominal efficiency of $\eta_{nom}^{GB} = 0.8$, *Figure 2c.* In the calculation, $\lambda^{GB}$ is set to $\lambda^{GB} = 0.2$ if $0.01 \leq \lambda^{GB} \leq 0.2$ and $\lambda^{GB} = 0.0$ if $\lambda^{GB} < 0.01$ to also consider the non-use of the gas boiler.

The electric boiler is calculated in the same way as the gas boiler. Thus, the thermal output $\dot{Q}^{EB}$ is determined according to

$$\dot{Q}^{EB} = \dot{Q}_{nom}^{EB} \lambda^{EB} \tag{10}$$

with the nominal capacity $\dot{Q}_{nom}^{EB}$ and the load fraction $0.0 \leq \lambda^{EB} \leq 1.0$. In contrast to the gas boiler, the entire range of the nominal capacity $\dot{Q}_{nom}^{EB}$ can be used. Furthermore, a constant efficiency $\eta^{EB} = 0.95$ is assumed, so that a required power is calculated by

$$P^{EB} = \frac{\dot{Q}^{EB}}{\eta^{EB}} = \frac{\dot{Q}^{EB}}{0.95}. \tag{11}$$

Finally, heat pumps are also considered for the heat supply, as these offer the possibility of providing heat very efficiently and on the basis of renewable energy sources, especially in connection with thermal energy storages and solar thermal systems. The thermal output $\dot{Q}^{HP}$ of the heat pump is also calculated by

$$\dot{Q}^{HP} = \dot{Q}_{nom}^{HP} \lambda^{HP} \tag{12}$$

with the nominal capacity $\dot{Q}_{nom}^{HP}$ and the load fraction $\lambda^{HP}$. As by the gas boilers, the load fraction is limited by an upper and lower bound, such that $0.2 \leq \lambda^{HP} \leq 1.0$. The efficiency of the heat pump is calculated according to [2] as the product of a constant 2nd law efficiency $\eta_{2nd}^{HP} = 0.36$ and the Carnot efficiency $\eta^{carnot}$ that serves as theoretical maximum:

$$\eta^{HP} = \eta_{2nd}^{HP} \eta^{carnot} = \eta_{2nd}^{HP} \frac{T_{h,out}^{HP}}{T_{h,out}^{HP} - T_{c,in}^{HP}} \tag{13}$$

with the heat sink temperature $T_{h,out}^{HP}$ as output and the heat source temperature $T_{c,in}^{HP}$ as input of the heat pump. In (13) it becomes clear that a heat pump can work most effective when an appropriate high-quality

heat source is available and the difference between $T_{h,out}^{HP}$ and $T_{c,in}^{HP}$ is as small as possible. The required electrical power $P^{HP}$ of the heat pump is then determined by

$$P^{HP} = \frac{\dot{Q}^{HP}}{\eta^{HP}}. \tag{14}$$

In addition to a minimum temperature difference of $T_{h,out}^{HP} - T_{c,in}^{HP} \geq 25K$ and a maximum output temperature $T_{h,out}^{HP} \leq 160°C$ are also taken into account, [9]. Using (13) and (14) the required thermal power $\dot{Q}_{TES}^{HP}$ taken from a connected thermal energy storage can be calculated for a given temperature difference:

$$\eta_{2nd}^{HP} \frac{T_{h,out}^{HP}}{T_{h,out}^{HP} - T_{c,in}^{HP}} = \frac{\dot{Q}^{HP}}{P^{HP}} = \frac{\dot{Q}^{HP}}{\dot{Q}^{HP} - \dot{Q}_{TES}^{HP}} \Longrightarrow \dot{Q}_{TES}^{HP} = \dot{Q}^{HP}\left(1 - \frac{T_{h,out}^{HP} - T_{c,in}^{HP}}{\eta_{2nd}^{HP} T_{h,out}^{HP}}\right). \tag{15}$$

Usually, only constant efficiencies of the heat pump are applied during the design process. However, this means that solar thermal unit, thermal energy storage and heat pump are considered separately, which can lead to an incorrect evaluation of the overall system.

## 2.3. Thermal energy storage

The thermal energy storage is used to store the thermal output generated by e.g. the solar thermal unit and to make it available for the generation of the required heat. It is used on the one hand for preheating but also as a source for the heat pump, *Figure 3a*. Starting from the currently stored thermal energy $Q_0^{TES}$, available thermal performance $\dot{Q}$ during the considered time frame $\Delta t$ is used to charge the storage tank

$$Q^{TES} = Q_0^{TES} + \dot{Q}\Delta t. \qquad \text{with} \qquad Q^{TES} \leq Q_{nom}^{TES} \tag{16}$$

ensuring that the nominal capacity $Q_{nom}^{TES}$ of storage is not exceeded. Due to the fact, only a hot water storage is used in this paper the temperature $T^{TES}$ of the storage tank can be determined based on the stored thermal energy $Q^{TES}$, the storage mass $m^{TES}$, the specific heat capacity of the storage medium $c_p^{TES}$ and initial temperature $T_0^{TES}$:

$$Q^{TES} = c_p^{TES} m^{TES}(T^{TES} - T_0^{TES}) \qquad \Longrightarrow \qquad T^{TES} = T_0^{TES} + \frac{Q^{TES}}{c_p^{TES} m^{TES}} \tag{17}$$

When discharging the storage, a simple calculation as in (16) is not suitable, because with the discharging of the storage, the storage temperature reduces and according to (15) also the thermal power taken from the storage by the heat pump. In order to be able to better describe the discharging, it is necessary to consider the power used for preheating $\dot{Q}_{TES}^{w}$ and for the heat pump $\dot{Q}_{TES}^{HP}$ within a single formulation

$$\dot{Q}^{TES} = -\dot{Q}_{TES}^{w} - \dot{Q}_{TES}^{HP} = -c_p^w \dot{m}^w (T^{TES} - \Delta T - T_{in}^w) + \dot{Q}^{HP}\left(\frac{T_{h,out}^{HP} - T^{TES}}{\eta_{2nd}^{HP} T_{h,out}^{HP}} - 1\right) \tag{18}$$

where the source temperature for the heat pump is set to the storage temperature $T_{c,in}^{HP} = T^{TES}$ and the output temperature for the preheating is chosen to be $T_{out}^{w} = T^{TES} - \Delta T$ in order to ensure a pinch in the heat exchangers of $\Delta T$. By rearranging (18), formulation

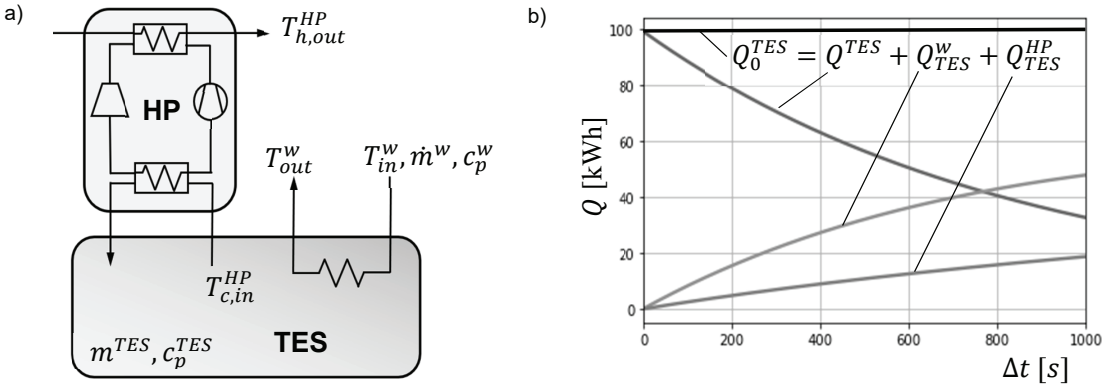


**Figure 3** description of the two options for discharging the storage (a) and discharging of the storage according to (22) using $m^{TES} = 1000kg$, $c_p^{TES} = 4.19\,kJ/kgK$, $T_0^{TES} = 15°C$, $c_p^w = 4.19\,kJ/kgK$, $\dot{m}^w = 1.0\,kg/s$, $\dot{Q}^{HP} = 100kW$ and $T_{h,out}^{HP} = 100°C$ (b)


https://doi.org/10.52202/069564-0123

$$\dot{Q}^{TES} = \underbrace{\left[c_p^w \dot{m}^w (\Delta T + T_{in}^w) + \dot{Q}^{HP}\left(\frac{T_{h,out}^{HP}}{\eta_{2nd}^{HP} T_{h,out}^{HP}} - 1\right)\right]}_{c_1} - \underbrace{\left[c_p^w \dot{m}^w + \frac{\dot{Q}^{HP}}{\eta_{2nd}^{HP} T_{h,out}^{HP}}\right]}_{c_2} T^{TES} \tag{19}$$

is obtained, where the terms in the square brackets, that are assumed to be constant with time, are summarized by the constants $c_1$ and $c_2$. If the formulation of $T^{TES}$ in (17) is used, equation (19) can be formulated such as

$$\dot{Q}^{TES} = c_1 - c_2 T^{TES} = c_1 - c_2\left(T_0^{TES} + \frac{Q^{TES}}{c_p^{TES} m^{TES}}\right) = \underbrace{c_1 - c_2 T_0^{TES}}_{c_3} - \underbrace{\frac{c_2}{c_p^{TES} m^{TES}}}_{c_4} Q^{TES} \tag{20}$$

with the constants $c_3$ and $c_4$, where (20) now depends on $Q^{TES}$. With this, the following problem can be formulated

$$\dot{Q}^{TES} = \frac{dQ^{TES}}{dt} = c_3 - c_4 Q^{TES} \qquad \Longrightarrow \qquad \frac{dQ^{TES}}{c_3 - c_4 Q^{TES}} = dt \tag{21}$$

which can be solved by integrating separately from $Q_0^{TES}$ to $Q^{TES}$ and $t_1$ to $t_2$, where $\Delta t = t_2 - t_1$:

$$Q^{TES} = \left(-\frac{c_3}{c_4} + Q_0^{TES}\right) e^{-c_4 \Delta t} + \frac{c_3}{c_4} \tag{22}$$

Using (22), the energy provided by the storage $Q^{TES} - Q_0^{TES}$ and $\dot{Q}_{TES}^{w}$ as well as $\dot{Q}_{TES}^{HP}$ can be calculated over different time ranges, taking into account the effect of (15) and the fact that also with decreasing storage temperature $T^{TES}$ in the preheating less energy can be transferred, *Figure3b*. During the discharging of the thermal energy storage it is checked that $Q^{TES} \geq 0$.

## 2.4. Integration of the components

To model the entire energy concept of the industrial process, the components described in the previous chapter must be integrated to check whether the demand of the production process can be covered at any time. The heat requirement considered here corresponds to the batch process of an existing food processing process shown in *Figure 4*a, whereby this is only applicable on weekdays, due to the fact that there is no production at off days. Here the day is divided into 7 sections, with different time periods $\Delta t^{(i)}$ and heat requirements $\dot{Q}^{dem,(i)}$ with a peak load that is only required for a short period of time.

For the analysis of the system consisting of the described components with their nominal capacity, representative weeks are evaluated for each month of the year. This is necessary because the solar radiation and thus also the power of the PV and ST unit change greatly over the course of a year. To determine the daily solar radiation $S_{\mathcal{M},d}^{hor}$ for a specific month, the monthly values $S_{\mathcal{M}}^{hor}$ are divided by the corresponding number of days per month. The analysis of each week starts on Saturday with an empty thermal energy storage. This means that the storage can be charged over the weekend, since there is no heat demand for the production process here. In general, the charging level of the storage is calculated according to the sections in *Figure 4a* by

$$Q^{TES,(i+1)} = Q^{TES,(i)} - \left(\dot{Q}_{TES}^{w,(i)} + \dot{Q}_{TES}^{HP,(i)} - \dot{Q}^{ST,(i)}\right)\Delta t^{(i)} \quad \text{w.r.t.} \quad Q^{TES,(i+1)} \leq Q_{nom}^{TES} \tag{23}$$

where at weekends $\dot{Q}_{TES}^{w,(i)} = \dot{Q}_{TES}^{HP,(i)} = 0$. In order to determine $\dot{Q}_{TES}^{HP,(i)}$, according to (18) it is necessary to define the thermal output of the heat pump $\dot{Q}^{HP}$. Since the components in the batch process under consideration have to be operated at partial load, in sections with a lower heat demand $\dot{Q}^{dem,(i)}$ it is necessary to determine appropriate load fractions $\lambda^{GB}, \lambda^{EB}$ and $\lambda^{HP}$ of the units. In this paper, this is realized by a load optimization with regard to minimal operating costs:

$$\min_{\boldsymbol{\lambda} \in L} f \qquad \text{s.t.} \qquad h = \dot{Q}^{dem,(i)} - \dot{Q}^{GB,(i)} - \dot{Q}^{EB,(i)} - \dot{Q}^{HP,(i)} - \dot{Q}_{TES}^{w,(i)} \leq 0 \tag{24}$$

with $f = p_{buy}^{el} E^{el,(i)} + p_{buy}^{gas} E^{gas,(i)}$, the price for electricity $p_{buy}^{el}$ and for natural gas $p_{buy}^{gas}$ as well as

$$E^{el,(i)} = \left(P^{HP,(i)} + P^{EB,(i)}\right)\Delta t^{(i)}, \qquad E^{gas,(i)} = P^{GB,(i)} \Delta t^{(i)}, \tag{25}$$

$$L = \{\boldsymbol{\lambda} = [\lambda^{GB}, \lambda^{EB}, \lambda^{HP}]^T \in \mathbb{R}^3 | h \leq 0, \boldsymbol{\lambda}^l \leq \boldsymbol{\lambda} \leq \boldsymbol{\lambda}^u\}. \tag{26}$$

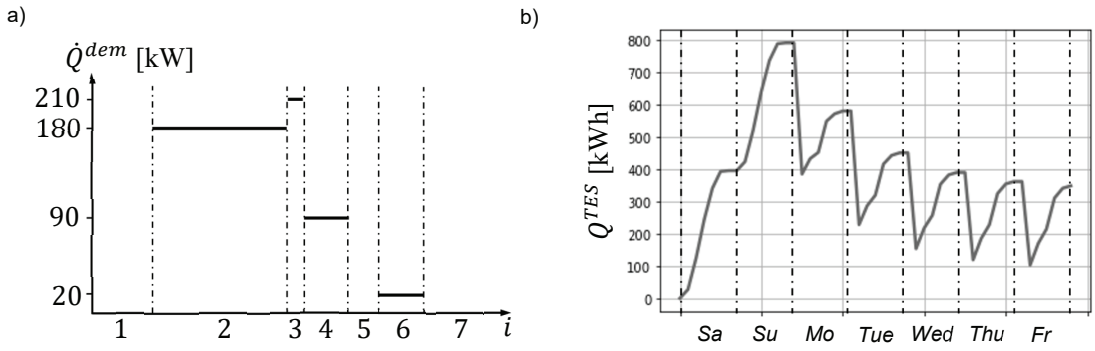


**Figure 4** a) considered batch process with daily heat demand sections $i$ and b) charging level of the thermal energy storage for one week in November and an exemplary energy concept

Due to $h \leq 0$ it can be ensured that the heat demand of the production process is covered with minimal operational cost. When calculating the required electrical energy $E^{el,(i)}$, the energy of the PV and WT unit is also taken into account, which is not required to cover the electricity demand of the production process. The total electricity demand of a day is then calculated according to

$$E_d^{el} = E_d^{BL} + E_d^{WL} - E_d^{PV} - E_d^{WT} + \sum_{j=1}^{7} \left( P^{HP,(j)} + P^{EB,(j)} \right) \Delta t^{(j)} \tag{27}$$

with daily energy generated by the PV unit $E_d^{PV}$ and the WT unit $E_d^{WT}$ as well as daily base load $E_d^{BL}$ and load $E_d^{WL}$ on the working days, which is needed e.g. to use the electrical machines. The daily gas demand is calculated according to

$$E_d^{gas} = \sum_{j=1}^{7} P^{GB,(j)} \Delta t^{(j)}. \tag{28}$$

The calculation of the daily demands is carried out consecutively for all days of the week. A negative energy demand means that more energy has been produced than is needed and this amount can be sold, a positive energy demand means that the corresponding amount has to be bought. The charging level of the storage is taken over from one day to the next, as shown exemplarily in *Figure 4b*. Since representative weeks with five working days are analysed for all months, a total of $4 \times 5 \times 12 = 240$ load optimizations (24) are required for an evaluation of the energy concept.

# 3. Deterministic optimization of the energy concept

The results of the analysis of the energy concept from section 2.4 essentially depend on the dimensioning or the nominal capacities of the units used. For example, larger PV or WT units lead to a larger amount of electrical energy being produced, which, according to (27), can reduce the energy demand. Furthermore, a larger ST unit with a corresponding thermal energy storage means that, according to (23), the heat pump also has a high-temperature source available or the energy in the storage can be used for preheating, so that less additional energy is needed. In addition, the $CO_2$ emissions can also be reduced by using renewable energy sources like PV, WT and ST units, although an increase in the normal capacities is also associated with increased investment costs. In order to find suitable trade-offs between economic criteria such as costs and ecological criteria such as $CO_2$ emissions, optimization processes are applied. Therefore, in the next section, the considered criteria will first be explained before the corresponding optimization problem is formulated and the optimization result is discussed.

## 3.1. Determination of the objectives

As already described, economic as well as ecological criteria are considered in the design process. The total annual costs $TAC$, which are calculated on the one hand from the required operating costs and on the other hand from the investment costs, are chosen as ecological criterion. The annual investment cost for each unit $c^i$ , $i \in \{PV, WT, ST, GB, EB, HP, TES\}$ is determined according to

$$c^i = \left( \frac{(\beta+1)^\tau \beta}{(\beta+1)^\tau - 1} + \alpha^i \right) C^i \qquad \text{with} \qquad C^i = C^{i,0} \left( \frac{\dot{Q}_{nom}^i / Q_{nom}^i / P_{nom}^i / A^i}{\dot{Q}_{nom}^{i,0} / Q_{nom}^{i,0} / P_{nom}^{i,0} / A^{i,0}} \right)^\gamma \tag{29}$$


https://doi.org/10.52202/069564-0123

with total capital expenditure $C^i$ for unit with nominal capacity $\dot{Q}^i_{nom}/Q^i_{nom}/P^i_{nom}/A^i$, cost $C^{i,0}$ and nominal capacity $\dot{Q}^{i,0}_{nom}/Q^{i,0}_{nom}/P^{i,0}_{nom}/A^{i,0}$ of a reference unit, scaling exponent $\gamma$, maintenance cost factor $\alpha^i$ and interest rate $\beta$ as well as time horizon $\tau$ at financing, [10]. Thus, in $c^i$ the annual rate for financing is combined with the maintenance costs. The values used here for the individual units are summarized in *Table 1*, [2], [11].

**Table 1** values for calculating annual component costs $c^i$

| | *reference capacity* | $CAPEX^0$[€] | $\gamma$ [−] | $\alpha$ [−] | $\tau$ [−] | $\beta$ [−] |
|---|---|---|---|---|---|---|
| PV unit | $P^{PV,0}_{nom} = 1$ kW | 1400 | 0.95 | 0.01 | 10 | 0.03 |
| WT unit | $P^{WT,0}_{nom} = 1$ kW | 5000 | 0.95 | 0.03 | 10 | 0.03 |
| ST unit | $A^{ST,0} = 1\ m^2$ | 240 | 0.95 | 0.5 | 10 | 0.03 |
| GB unit | $\dot{Q}^{GB,0}_{nom} = 1$ kW | 2700 | 0.45 | 0.015 | 10 | 0.03 |
| EB system | $\dot{Q}^{EB,0}_{nom} = 1$ kW | 70 | 0.66 | 0.02 | 10 | 0.03 |
| HP system | $P^{HP,0}_{nom} = 1$ kW | 2650 | 0.95 | 0.02 | 10 | 0.03 |
| TES system | $Q^{TES,0}_{nom} = 1$ kWh | 80 | 0.87 | 0.02 | 10 | 0.03 |

To calculate the operating costs, days with positive and negative energy demand $E^{el}_d$ must be considered separately. Thus, in $E^{el}_{in,m}$, all positive energy demands of the considered representative week of each month $m$ are summarized and in $E^{el}_{out,m}$ all negative ones. For the calculation of the weekly gas demand $E^{gas}_{in,m}$, however, the daily values $E^{gas}_d$ are simply summed up. The total annual costs $TAC$ can then be calculated:

$$TAC = \sum_{m\in\mathcal{M}} \left(p^{el}_{buy}E^{el}_{in,m} - p^{el}_{sell}E^{el}_{out,m} + p^{gas}_{buy}E^{gas}_{in,m}\right)4.3 + \sum_{i\in\Im} c^i \tag{30}$$

with $\mathcal{M} = \{Jan,\ Feb,\ \cdots,\ Dec\}$, $\Im = \{PV, WT, ST, GB, EB, HP, TES\}$, revenue for the sale $p^{el}_{sell} = 0.06\ €/\text{kW}$ and price for the purchase $p^{el}_{buy} = 0.35\ €/\text{kW}$ of electrical energy as well as price for natural gas $p^{gas}_{buy} = 0.13\ €/\text{kW}$. The weekly values are multiplied by 4.3 to get estimated monthly values.

The global warming impact $GWI$ is considered as ecological criterion

$$GWI = \sum_{m\in\mathcal{M}} \left(g^{el}\left(E^{el}_{in,m} - E^{el}_{out,m}\right) + g^{gas}E^{gas}_{in,m}\right) \tag{31}$$

with the specific global warming impacts $g^{el} = 349\ \text{g}_{\text{CO2eq}}/\text{kWh}$ and $g^{gas} = 244\ \text{g}_{\text{CO2eq}}/\text{kWh}$ of electricity and natural gas, respectively [2]. It should be noted that the specific global warming impact from purchased energy is actually varying greatly over time, depending on the shares of e.g. renewable energies. Formulation (31) reduces the $GWI$ through the purchase of energy to emphasize the positive contribution. It should be noted at this point that the manufacture of components or units also has an effect on the $GWI$, which, according to [12], is significantly lower than that caused by operation. However, the contribution of manufacturing to the $GWI$ is not considered here.

## 3.2. Optimization problem formulation

The two optimization objectives (30) and (31) depend on the one hand on the investment costs of the installed units and on the other hand on the consumption of electrical energy and natural gas. Both criteria therefore depend on the nominal capacities of the installed units, which are to be determined as part of an optimal design. Thus, the design parameters $\mathbf{p}_{nom}$ of the energy concept are:

$$\mathbf{p}_{nom} = \left[A^{PV}, P^{WT}_{nom}, A^{ST}, \dot{Q}^{GB}_{nom}, \dot{Q}^{EB}_{nom}, \dot{Q}^{HP}_{nom}, Q^{TES}_{nom}\right]^T. \tag{32}$$

The multi-objective optimization problem for minimizing both objectives simultaneously is

$$\min_{\mathbf{p}_{nom}\in P} \begin{bmatrix} TAC \\ GWI \end{bmatrix} \qquad \text{with} \qquad P = \{\mathbf{p}_{nom} \in \mathbb{R}^7 | h_{max} \le 0, \mathbf{p}^l_{nom} \le \mathbf{p}_{nom} \le \mathbf{p}^u_{nom}\} \tag{33}$$

with the constraint $h_{max} = max\left(\dot{Q}^{dem,(i)} - \dot{Q}^{GB,(i)} - \dot{Q}^{EB,(i)} - \dot{Q}^{HP,(i)}\right)$, which is the maximum of all constraints $h$ of the optimal solution of the problem (24). It can happen, that if the nominal capacities of the GB, EB and HP units are chosen too small, a valid solution of (24) is not possible, which result in $h > 0$. This constraint is essential, since the units are chosen to be as small as possible, particularly to reduce the investment costs. The lower limits for the design parameters are chosen to be $\mathbf{p}^l_{nom} = [0, 0, 0, 0, 0, 0, 0]^T$ and the upper limits to be $\mathbf{p}^u_{nom} = [4000, 24, 2000, 250, 250, 250,\ 5000]^T$. This means that individual units do

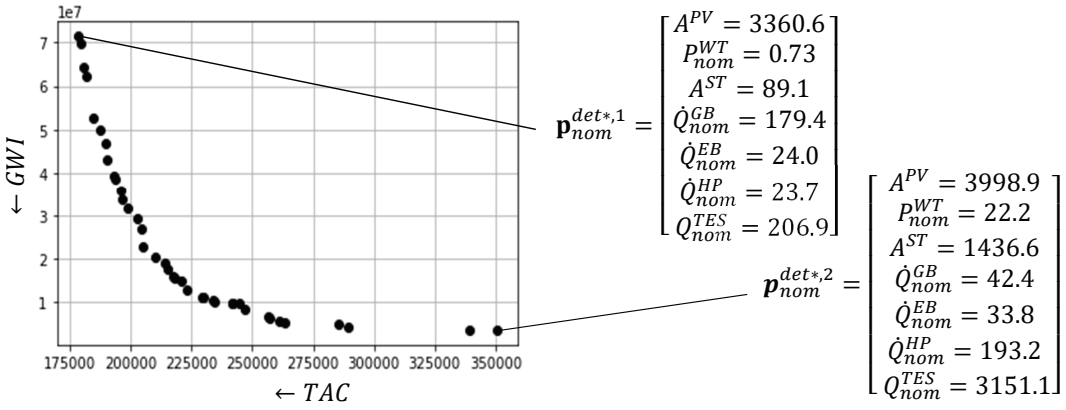


**Figure 5** Pareto-front as solution of the multi-objective problem (33)

not have to be used and the entire heat requirement can be covered by GB, EB or HP. It should be noted here that the capacity of the units is modelled continuously, so that the results may not be directly implemented in practice, since e.g. PV units are only available in a certain size.

### 3.3. Discussion of the results

The optimization problem (33) is solved by the genetic algorithm NSGA2 which is implemented like the modelling of the units and the energy concept in Python, [13]. The result is a Pareto-front consisting of optimal compromises between the objectives, *Figure 5.* Here it can be clearly seen that the objectives $TAC$ and $GWI$ are contradictory and the design $\mathbf{p}_{nom}^{det*,1}$ for a minimum $TAC$ causes only about half the annual costs as the design $\boldsymbol{p}_{nom}^{det*,2}$ for a minimum $GWI$. However, there are also compromises in between that can be chosen for implementation. The low $TAC$ is realized mainly due to a low gas price $p_{buy}^{gas}$ compared to the price of electricity $p_{buy}^{el}$ and a high nominal capacity $\dot{Q}_{nom}^{GB}$ of the GB unit, while a low $GWI$ is achieved through a high use of renewable energy sources, a large thermal energy storage and a high nominal capacity $\dot{Q}_{nom}^{HP}$ of the HP unit.

## 4. Robust optimization approach

The result of the optimization from chapter 3.3 depend decisively on the assumptions about e.g. prices for electricity and gas, unit performances, investment costs as well as assumptions about environmental influences such as wind speeds and solar radiation. Uncertainties in these assumptions can lead to deviating and undesirable system behaviour. It is the task of robust optimization to take this into account in the design process. In the following sections, the uncertainties assumed here are presented, the corresponding robust optimization concept is explained and finally the solution from deterministic and robust optimization is compared.

### 4.1. Description of uncertainties

In this paper uncertainties in the price of gas $p_{buy}^{gas}$ and in the solar radiation $S^{pan}$ on the panels are considered for a first investigation. This is realized in the form of two uncertainty factors $f_1$ and $f_2$ such that:

$$\tilde{S}^{pan} = S^{pan} f_1 \qquad \text{and} \qquad \tilde{p}_{buy}^{gas} = p_{buy}^{gas} f_2 \tag{34}$$

with $0.9 \leq f_1 \leq 1.0$ and $1.0 \leq f_2 \leq 2.0$. Thus, the gas price will change with an assumed increase of up to $100\%$. Solar radiation is assumed to be reduced by up to $10\%$, which corresponds to degraded panel performance, additional shading, or overestimation of solar radiation.

Local response surfaces are used to assess the influence of $f_1$ and $f_2$ on the optimization objectives (30) and (31), [14]. Response surfaces enable the relationship between input parameters and output of a function to be approximated on the basis of a few function evaluations in order to subsequently carrying out extensive statistical studies very efficiently. To set up the response surfaces, a random sample $\left[f_1^{(i)}, f_2^{(i)}\right], i = 1(1)4$ based on a Latin Hypercube Sampling is defined and analysed with $\mathbf{p}_{nom} = \mathbf{p}_{nom}^{det*,1} = const.$ Kriging models $\hat{y}_{TAC}$ and $\hat{y}_{GWI}$ are then created using the calculated values of $TAC^{(i)}$ and $GWI^{(i)}$, [15]. The response surface $\hat{y}_{TAC}$ is shown in *Figure 6a* as an example. A sample with $N = 1e3$ sampling points is then defined and


https://doi.org/10.52202/069564-0123

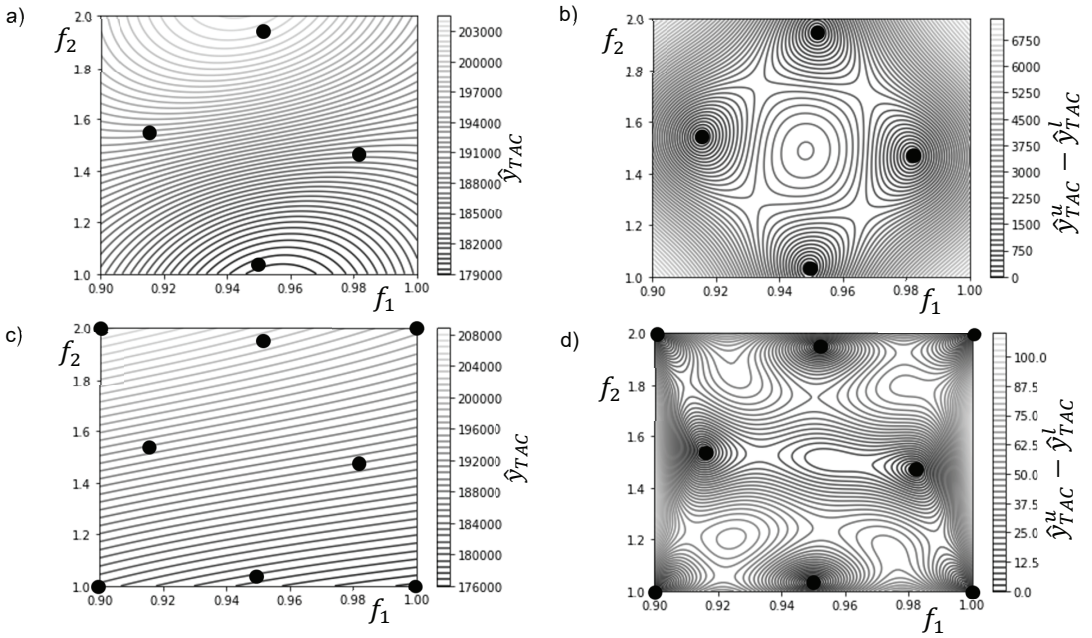


**Figure 6** approximation of $\hat{y}_{TAC}$ using a) four and c) eight design evaluations (●) and the associated differences $\hat{y}^u_{TAC} - \hat{y}^l_{TAC}$ between upper and lower bound (b) and (d)

evaluated just using the response surfaces in order to determine the robust criteria. The $95\%$ quantiles $P^{TAC}_{95}$ and $P^{GWI}_{95}$ of the objectives are chosen as criteria, which e.g. for $TAC$ is defined as follows:

$$\frac{1}{N}\sum_{i=1}^{N} I(\hat{y}^{(i)}_{TAC}) = 0.95 \qquad \text{with} \qquad I(\hat{y}^{(i)}_{TAC}) = \begin{cases} 1 & \hat{y}^{(i)}_{TAC} \le P^{TAC}_{95} \\ 0 & else \end{cases}, \tag{35}$$

and describes a value under which $95\%$ of all elements of the sample are located. However, since the criteria were only determined on the basis of the response surfaces, the question arises as to how accurate these estimates were. For this purpose, the variances $\hat{s}_{TAC}$ and $\hat{s}_{GWI}$ of the Kriging estimates $\hat{y}_{TAC}$ and $\hat{y}_{GWI}$ can be used, [16]. This allows to define lower and upper limits, e.g.

$$\hat{y}^{l,(i)}_{TAC} = \hat{y}^{(i)}_{TAC} - 3\hat{s}^{(i)}_{TAC} \qquad \text{and} \qquad \hat{y}^{u,(i)}_{TAC} = \hat{y}^{(i)}_{TAC} + 3\hat{s}^{(i)}_{TAC}\,, \tag{36}$$

which define a range in which the actual value $TAC^{(i)}$ is within a probability of $\approx 99.99\%$, *Figure 6b*. With these lower and upper limits, the quantiles can then be determined according to (35) and thus a quantile range

$$R^{TAC}_{P,95} = P^{u,TAC}_{95} - P^{l,TAC}_{95} \tag{37}$$

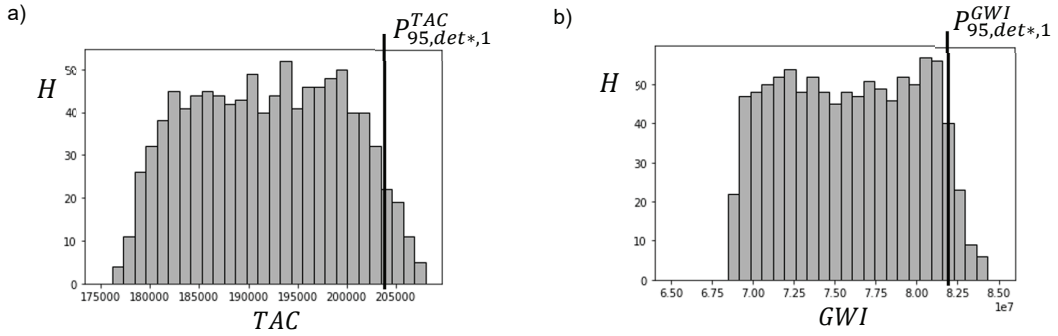


**Figure 7** frequency distributions of the optimal solution $\boldsymbol{p}^{det*,1}_{nom}$ with respect to a) $TAC$ and b) $GWI$

can be estimated. If this range is above a $1\%$ limit of $P_{95}^{TAC}$, the response surface has to be refined. Appropriate update points are defined by solving the optimization problem

$$\max_{f_1,f_2} \hat{s}_{TAC} \qquad \text{with} \qquad 0.9 \leq f_1 \leq 1.0 \qquad \text{and} \quad 1.0 \leq f_2 \leq 2.0 \tag{38}$$

which finds the point where the estimation $\hat{y}_{TAC}$ has the greatest variance $\hat{s}_{TAC}$. This update process is carried out until the quantile range (37) is sufficiently small, *Figure 6c* and *d*. As can be seen, the response surface can thus be updated very efficiently using just a few iterations. The distributions and estimates for the quantiles $P_{95,det*,1}^{TAC}$ and $P_{95,det*,1}^{GWI}$ determined for the design $\mathbf{p}_{nom}^{det*,1}$ for minimal $TAC$ using the updated response surfaces are shown exemplarily in *Figure 7,* where the spread in the $TAC$ covers a range of $30\text{k€}$.

## 4.2. Robust optimization concept

As reference for the robust optimization the optimal design $\mathbf{p}_{nom}^{det*,1}$ of the deterministic optimization (33) is chosen, because it may be an appropriate choice from an economic perspective. Due to the fact, that the robust assessment is performed according to the adaptive local response surface procedure described in the previous section, where a number of energy concept evaluations are needed for a single design, just a single objective robust optimization approach is chosen in order to reduce the computational effort. This results in the optimization problem

$$\min_{\mathbf{p}_{nom} \in P} P_{95}^{TAC} \quad \text{with} \quad P = \left\{ \mathbf{p}_{nom} \in \mathbb{R}^7 \left| \begin{bmatrix} h_{max} \\ P_{95}^{GWI} - P_{95,det*,1}^{GWI} \end{bmatrix} \leq \mathbf{0}, \mathbf{p}_{nom}^{l} \leq \mathbf{p}_{nom} \leq \mathbf{p}_{nom}^{u} \right. \right\}, \tag{39}$$

where in addition to (33) a further constraint is added to ensure that an improvement of $P_{95}^{TAC}$ is not be achieved by an increase of $P_{95}^{GWI}$ and a comparability with the design $\mathbf{p}_{nom}^{det*,1}$ can be guaranteed.

## 4.3. Comparison of optimization results

The optimization problem (39) is solved using a differential evolution algorithm implemented in Python, whereby the computing time was approximately twice as high as with the deterministic multi-objective optimization (33). In contrast to multi-objective optimization, the result is not a set of optimal compromises but a single design

$$\begin{aligned} \boldsymbol{p}_{nom}^{rob*} &= \left[A^{PV}, P_{nom}^{WT}, A^{ST}, \dot{Q}_{nom}^{GB}, \dot{Q}_{nom}^{EB}, \dot{Q}_{nom}^{HP}, Q_{nom}^{TES}\right]^T \\ &= [3539.7,\ 0.3,\ 173.7,\ 3.5,\ 57.6,\ 161.9,\ 755.3]^T. \end{aligned} \tag{40}$$

Compared to the deterministic optimum $\mathbf{p}_{nom}^{det*,1}$, *Figure 5*, the TES and the ST unit were significantly increased and the nominal capacity of the GB unit was reduced to a small value. According to the selected robust criterion, the quantile value $P_{95}^{TAC}$ and thus the high costs to be expected could be reduced, *Figure 8a*. However, over a wide range, the deterministic optimum $\mathbf{p}_{nom}^{det*,1}$ results in low $TAC$, whereas the robust optimum has a significantly smaller variance in the $TAC$. In any case, the robust optimum $\boldsymbol{p}_{nom}^{rob*}$ results in a significantly smaller $GWI$, *Figure 8b,* which was not a goal of the optimization but is an effect due to an increase in the share of renewable energies. The choice of a specific objective of the robust optimization or the desired properties of the energy concept depend heavily on individual factors and must be redetermined depending on the situation.

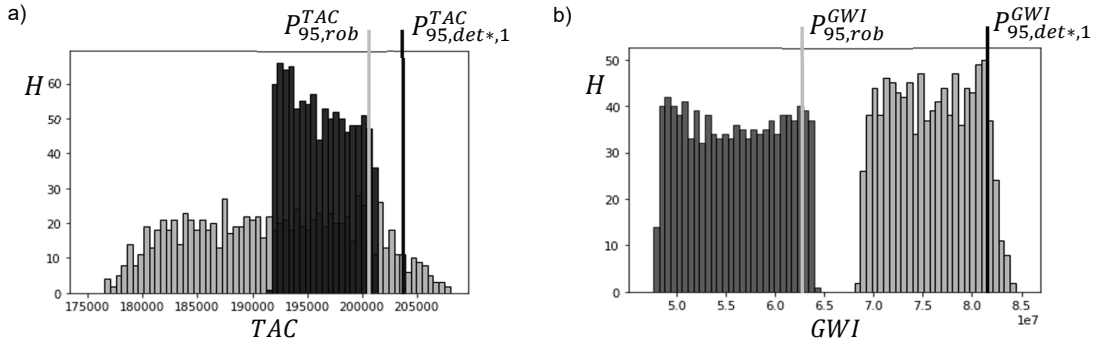


**Figure 8** frequency distributions of the optimal solutions $\boldsymbol{p}_{nom}^{det*,1}$ (grey) and $\boldsymbol{p}_{nom}^{rob*}$ (dark grey) with respect to a) $TAC$ and b) $GWI$


https://doi.org/10.52202/069564-0123

## 5. Conclusions

In this paper, the modelling of units of an energy concept was described and the procedure for the integrated analysis with regard to economic and environmental criteria was explained. Based on the analysis, a deterministic multi-objective and a robust single-objective optimization problem for the dimensioning of the units used were defined and corresponding optimizations were carried out.

It turns out that the results of the deterministic optimization depend strongly on the assumptions and boundary conditions used and deviations can lead to a large scatter in the objective functions. Furthermore, changes in the boundary conditions of the optimization can lead to different optimal configurations. As part of a robust optimization, assumptions about uncertainties in the price of natural gas and the solar radiation were considered and a design was found that has a lower scatter in the $TAC$ and reduces the expected high costs compared to a selected reference design from the deterministic multi-objective optimization. This shows that the consideration of uncertainties is particularly necessary for long planning periods. In general, the result of a robust optimization strongly depends on the criteria and uncertainties considered, so that different criteria and more realistic assumptions of the uncertainties are investigated in further studies.

## References


[1] P. Voll, C. Klaffke, M. Hennen and A Bardow: Automated Superstructure-based Synthesis and Optimization of Distributed Energy Supply Systems. *Energy*, Volume 50, pp. 374-388, 2013.

[2] S. Sass, T. Faulwasser, D.E. Hollermann, C.D. Kappatou, D. Sauer, T. Schütz, D.Y. Shu, A. Bardow, L. Gröll, V. Hagenmeyer, D. Müller and A. Mitsos: Model Compendium, Data and Optimization Benchmarks for Sector-Coupled Energy Systems. *Computers and Chemical Engineering*, Volume 135, 106760, 2020.

[3] A.J. Keane and P.B. Nair: Computational Approaches in Aerospace Design, The Pursuit to Excellence. *John Wiley & Sons*, New York, 2005.

[4] D.E. Majewski, M. Wirtz, M. Lampe and A. Bardow: Robust Multi-Objective Optimization for Sustainable Design of distributed Energy Supply Systems. *Computers and Chemical Engineering*, Volume *102*, pp. 26-39, 2017.

[5] G. Dellino, J.P.C. Kleijnen and C. Meloni: Robust Optimization in Simulation: Taguchi and Response Surface Methodology. *International Journal of Production Economics*, Volume 125 (1), pp. 52-59, 2010.

[6] DWD – Deutscher Wetter Dienst: Average 30-Year Monthly and Annual Sums of Global Radiation – *available at: https://www.dwd.de/DE/leistungen/solarenergie/strahlungskarten_mvs.html?nn=16102* [accesed 13.03.2023]

[7] R. Debulac, S. Serra, S. Sochard and J.-M. Reneaume: A Dynamic Optimization Tool to Size and Operate Solar Thermal District Heating Networks Production Plants. *Energies*, Volume 14, 8003, 2021.

[8] G.B. Murphy, M. Kummert, B.R. Anderson and J. Counsell: A Comparision of the UK Standard Assessment Proceure (SAP) and detailed Simulation of Building-integrated Renewable Energy Systems. *Journal of Building Performance Simulation*, Volume 4 (1), pp.75-90, 2011.

[9] F. Schlosser, M. Jesper, J. Vogelsang, T.G. Walmsley, C. Arpagaus and J. Hesselbach: Large-scale Heat pumps: Applications, Performance, Economic Feasibility and Industrial Integration. *Renewable and Sustainable Energy Reviews*, Volume 133, 110219, 2020.

[10] R. Smith: Chemical Process: Design and Integration. *John Wiley & Sons*, Chichester, 2005.

[11] M. Seitz, H. von Storch, A. Nechache and D. Bauer: Techno Economic Design of a Solid Oxide Electrolysis System with Solar Thermal Steam Supply and Thermal Energy Storage for the Generation of Renewable Hydrogen. *International Journal of Hydrogen Energy*, Volume 42 (42), pp. 26192-26202, 2017.

[12] G. Guillèn-Gosálbez: A noval MILP-based Objective Reduction Method for Multi-Objective Optimization: Application to Environmental Problems. *Computers and Chemical Engineering*, Volume 35 (8), pp. 1469-1477, 2011.

[13] K. Deb, S. Agrawal, A. Pratap and T. Meyarivan: A Fast Elitist Non-Dominated Sorting Genetic Algorithm for Multi-Objective Optmization: NSGAII. *Proceedings of the 6th International Conference on Parallel Problem Solving from Nature*, Paris, France, pp. 849-858, 2000.

[14] D. Bestle, P. Flassig and A.K. Dutta: *Optimal* Aerodynamik Compressor Blade Design Considering Manufacturing Noise. *Proceedings of the 9th European Conference on Turbomachinery*, Istanbul, Turkey, 2011.

[15] D.R. Jones, M. Schonlau and W.J. Welch: Efficient Global Optimization of Expensive Black-Box Functions. *Journal of Global Optimization*, Volume 13, pp. 455-492, 1998.

[16] D.R. Jones: A Taxonomy of Global Optimization Methods based on Response Surfaces. *Journal of Global Optimization*, Volume 21, pp. 348-383, 2001.